

Application of a Double Layer Circular Microchannel Heat Sink in Electronic Industry

Sagar M. Narayanan, Pradeep M. Kamath



Abstract—The present paper is focused to evaluate the pressure drop and heat transfer performance of a double layer circular microchannel heat sink with numerically and experimentally. Numerical analysis is carried for various mass flow rates, with turbulent condition used in the ANSYS Fluent for two flow arrangements. The experiment is carried out by varying the mass flow rate ranges 3.32×10^{-4} kg/s to 27.72×10^{-4} kg/s with water as the cooling medium. The effect of a parallel flow and counter flow arrangements on heat transfer and flow parameters is studied for a constant heat input of 80W. The numerical result is nearly the same with the measured values. The pressure drop increases with the mass flow rate. The heat transfer enhancement is evaluated by the wall surface temperature and temperature uniformity. Even though parallel and counter flow arrangement has similar flow and thermal behavior, the latter has better temperature uniformity in the base of the heat sink for all pumping powers.

Keywords: Circular micro channel, counter flow, double layer, experiment, numerical, parallel flow.

I. INTRODUCTION

Miniaturization of electronic chips and technological advancement in them has tremendously increased the heat load. High heat removal is essentially required to maintain the chip surface temperature within the operating temperatures. Microchannel cooling is a promising solution.

Tuckerman and Pease [1] introduced the micro channel heat sink for the cooling purpose by using a rectangular microchannel heat sink (MCHS) of $1 \times 1 \text{ cm}^2$ silicon wafer. Since then the thermal performance improvement has been studied by many authors using different geometries. Adams et al. [2] conducted the study of forced convection in circular micro channels of 0.76 and 1.09 mm diameter with water as the cooling medium and compared with previous results. The discrepancy with observed values and the foresee Nu numbers is less for 1.09 mm diameter microchannel than the 0.76 mm microchannel.

Qu and Mudawar[3] numerically and experimentally observed the thermal performance of a $231 \mu\text{m}$ wide and $713 \mu\text{m}$ deep microchannel for two heat flux levels of 100 W/cm^2 (for Re 139 – 1672) and 200 W/cm^2 (for Re 385 – 1289). The observed pressure drop and the temperature variations have insignificant change with the numerical values. Soheli et al. [4]

investigated about thermal analysis and thermo physics with three different nano fluids like Al_2O_3 -water, Ti_2O_3 -water and CuO-water passing through a circular microchannel. Results show that CuO-water nanoparticles have better thermal enhancements at higher Reynolds number.

Sahar et al. [5] numerically studied the pressure drop and heat transfer enhancement in a metallic rectangular cross-section microchannel. The result shows the transition from laminar occurs in between Reynolds number 1600- 2000. Naphan et al. [6] experimentally analyzed the heat transfer characteristics in an MCHS having a different cross-section. The shape and size of the roughness irregularities depend on the heat transfer and flow characteristics. Owahib and Palm [7] conducted their work with convective heat transfer in circular micro channels of radius 0.85 mm, 0.6 mm, and 0.4 mm. In the turbulent region, the values similar to classical correlation and in laminar regime the heat transfer coefficients were identical for all three diameters.

Li et.al [8] perceives the thermal and hydraulic exposure of smooth microtube. Simulations carried out with k-ε model and result found to be varying between $\pm 10\%$ error bands. The increase in the wall temperature of the single-layer design is reduced with pressure. Many investigators studied the performance in double-layer micro channels.

Vafai and Zhu [9] investigated the thermal aspects of a double layer microchannel heat sink (DL-MCHS). Compared to the single layered microchannel heat sink (SL-MCHS) DL-MCHS needs lesser pressure drop and pumping power. The main purpose of implementing double layer microchannel is also to lower the temperature rise through axial direction. In this study, the better thermal analysis occurred for parallel flow (PF) arrangement than counter flow (CF) arrangement. Dede and Liu [10] numerically and experimentally studied the effect of multi-pass branching in MCHS for different flow rates with low-pressure drop and large heat fluxes. The experimental results of the heat and flow performances with latest design have similar outcome with the numerical and analytical data.

Lei et al. [11] conducted the numerical and experimental studies on a single and double layered square mini channel heat sink.

Revised Manuscript Received on October 30, 2019.

* Correspondence Author

Sagar M. Narayanan*, Research Scholar, Department Of Mechanical Engineering, Government Engineering College, Thrissur, Kerala, India. Email:sagar.narayanan@gmail.com

Pradeep M. Kamath, Assistant Professor, Department Of Mechanical Engineering, Government Engineering College, Thrissur, Kerala, India Email: pradeepmkamath@gmail.com

© The Authors. Published by Blue Eyes Intelligence Engineering and Sciences Publication (BEIESP). This is an open access article under the CC-BY-NC-ND license <http://creativecommons.org/licenses/by-nc-nd/4.0/>



The multilayered design is more efficient than the single layer design. Osanloo et al. [12] numerically perceive the performance of a DLMCHS with both lower and upper channel tapered. They validated the results with those attain from the literature. Zhai et al. [13] numerically analyzed the temperature distribution in each layer of a DL configuration with a parallel flow (PF) and counterflow (CF) arrangement. The result shows that the temperature increases along the flow direction in the PF arrangement.

In the case of CF arrangement the temperature rises initially along the direction of flow and reaching a maximum and then decreases.

The review of the literature shows that several numerical studies were conducted in microchannel but experimental studies were limited. Experimental studies with circular double-layer microchannel were found to be scarce. Important aim of the present work is to analyze the flow and thermal performance of a stacked double layer circular microchannel heat sink numerically and experimentally with the counter flow (CF) and parallel flow (PF) arrangement.

The present study is divided into two sections 1. Numerical analysis: 2. Experimental analysis:

II. NUMERICAL ANALYSIS

Figure 1 represents the schematic diagram of the computational domain used in the numerical analysis. The lower portion is a heat source and the upper portion is a heat sink. Half of the geometry is taken for the analysis due to the symmetry of the problem. The 10 micro channels arranged in two layers. The channel length is 20 mm and the size of the heat source block is 38 x 38 x 10 mm.

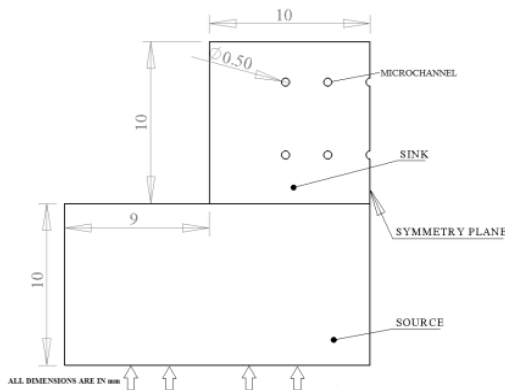


Fig. 1. Numerical model symmetry

The conservation equations for the fluid flow and heat transfer for solving the model are as follows.

Equation of continuity,

$$\frac{\partial u}{\partial x} + \frac{\partial v}{\partial y} + \frac{\partial w}{\partial z} = 0 \quad (1)$$

Equation of momentum,

$$\begin{aligned} \rho \left(u \frac{\partial u}{\partial x} + v \frac{\partial u}{\partial y} + w \frac{\partial u}{\partial z} \right) &= -\frac{\partial p}{\partial x} + \mu \left(\frac{\partial^2 u}{\partial x^2} + \frac{\partial^2 u}{\partial y^2} + \frac{\partial^2 u}{\partial z^2} \right) \\ \rho \left(u \frac{\partial v}{\partial x} + v \frac{\partial v}{\partial y} + w \frac{\partial v}{\partial z} \right) &= -\frac{\partial p}{\partial y} + \mu \left(\frac{\partial^2 v}{\partial x^2} + \frac{\partial^2 v}{\partial y^2} + \frac{\partial^2 v}{\partial z^2} \right) \\ \rho \left(u \frac{\partial w}{\partial x} + v \frac{\partial w}{\partial y} + w \frac{\partial w}{\partial z} \right) &= -\frac{\partial p}{\partial z} + \mu \left(\frac{\partial^2 w}{\partial x^2} + \frac{\partial^2 w}{\partial y^2} + \frac{\partial^2 w}{\partial z^2} \right) \end{aligned} \quad (2)$$

Equation of energy for solid,

$$\left(\frac{\partial^2 T_s}{\partial x^2} + \frac{\partial^2 T_s}{\partial y^2} + \frac{\partial^2 T_s}{\partial z^2} \right) = 0 \quad (3)$$

Equation of energy for fluid,

$$\rho C \left(u \frac{\partial T}{\partial x} + v \frac{\partial T}{\partial y} + w \frac{\partial T}{\partial z} \right) = k \left(\frac{\partial^2 T}{\partial x^2} + \frac{\partial^2 T}{\partial y^2} + \frac{\partial^2 T}{\partial z^2} \right) \quad (4)$$

Transport equations (k- ω Model) are [14]

$$\frac{\partial}{\partial t} [\rho k] + \frac{\partial}{\partial x_i} [\rho k u_i] = \frac{\partial}{\partial x_j} \left[\Gamma_k \frac{\partial k}{\partial x_j} \right] + G_k - Y_k \quad (5)$$

$$\frac{\partial}{\partial t} [\rho \omega] + \frac{\partial}{\partial x_i} [\rho \omega u_i] = \frac{\partial}{\partial x_j} \left[\Gamma_\omega \frac{\partial \omega}{\partial x_j} \right] + G_\omega - Y_\omega \quad (6)$$

The above governing equations are solved by using commercial software Ansys Fluent. The following are the boundary conditions used for the simulation. At inlet uniform inlet velocity and at outlet pressure outlet conditions are given. The inlet temperature is set as 303 K. Assuming water flows through the channel. Numerical analysis is conducted for mass flow rate ranging from 3.33×10^{-4} kg/s to 25.6×10^{-4} kg/s. A residual of 10^{-7} is set as convergence criteria for all equations. At the bottom of source block, a consistent of 55401 W/m^2 (corresponding to 80W) heat flux is applied. The heat sink top is assumed as convective with coefficient of heat transfer $12 \text{ W/m}^2\text{K}$. All other walls have a coefficient of convective heat transfer of $8 \text{ W/m}^2\text{K}$. The assumptions made are steady-state, incompressible, single phase, turbulent flow with constant thermophysical properties for fluid and solid. No slip boundary condition applied at the solid-fluid interface. The model used to simulate is standard k- ω .

Table1. Grid independence study

| Mesh Quality | Number of Nodes | Outlet Temperature(K) | % Change |
|--------------|-----------------|-----------------------|----------|
| Very coarse | 1002297 | 308.836 | --- |
| Coarse | 2071409 | 308.814 | 0.0071 |
| Fine | 4756507 | 308.806 | 0.0025 |
| Superfine | 8876049 | 308.782 | 0.0077 |

The grid independence study is carried out for the mass flow rate of 3.32×10^{-4} kg/s. Four different meshes are analyzed as shown in Table 1. The nodes correspond to the fine mesh is used for the present analysis.

III. EXPERIMENTAL SETUP

The set up of the experiment include with a double layered circular microchannel machined on a copper block having poly-tetra-fluoro-ethylene (Teflon) insulation on all except top surface, so as to minimize the heat losses.

The Figure 2 represents the schematic of experimental setup. It involves a constant temperature bath, test section, data acquisition system, peristaltic pump, DC power supply, and a computer.



The detailed view of the copper test section with a Teflon cover is shown in Figure 3. The photography of the actual experiment set up is shown in Figure 4. Direct Q-make water demineralization and purification system are used to de-ionize the water and a 5-micron filter is used to filter out the impurities. The filtered water is then stored in a constant temperature bath. The test section consist of a copper block which consists of two parts namely heat sink and heat source machine on a single square copper bar. The heat sink consists of ten micro channels with 700 μm diameter machined by WIRE EDM method. Micro channels are arranged in two layers on the upper portion of the copper block, one over the other. There are five channels in lower and upper layer. Continuous flow through the double layered microchannel is ensured with the help of two peristaltic pumps (range 0.035 ml/min - 2280 ml/min). The mass flow rate (MFR) is controlled by varying rpm of the peristaltic pump. Two pressure transducers (ranges 0-2.5 bar and an output of 1-5 Volts) are used to note inlet and outlet microchannel pressures. Four cartridge heaters are connected equally symmetric from the bottom portion of the heat source. They are connected to four Key Sight U8001 A (0-30V, 3A) DC Power Supply. Thermal paste is given on the outer side of the cartridge heaters to decrease the contact resistance. Total 80 W heat input is given to the heat sink by using these four cartridge heaters.

The heat sink is covered on all the sides except the top surface by Teflon block. Inlet and outlet plenums are cut in two Teflon blocks. The temperature at different locations is measured with calibrated 0.8 mm diameter K- type thermocouple. An Armature Multiplexer Module with 20 channels is used to connect all the thermocouples and the pressure lines with the data acquisition switch unit. Agilent 34970A DAQ is connected to measure all the data to the computer with the USB/GPIB interface.

The apparatus is permitted to run continuously for sufficient time to reach a steady state. Assuming a steady state condition of outlet temperature of the water is changed less than 0.1°C in ten minutes. All the readings are taken at this condition. In the present study, both PF and CF arrangements are experimentally investigated for different MFR. The heat loss is calculated using Fourier's law of heat conduction. It is found to be less than 9%. The measurement uncertainty in the radius of the microchannel and temperature is ± 0.03 mm and 0.1°C respectively. The measurement uncertainty of the pressure transducer is 1.5% of full-scale.

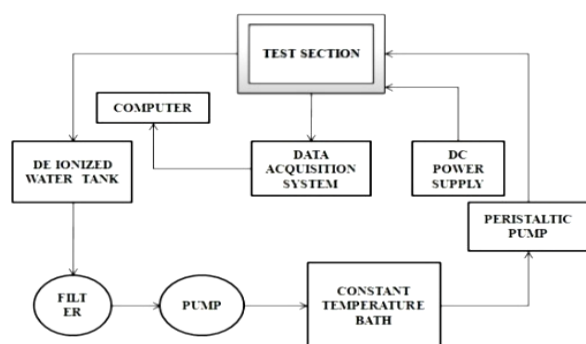


Fig. 2. Schematic diagram for the experiment

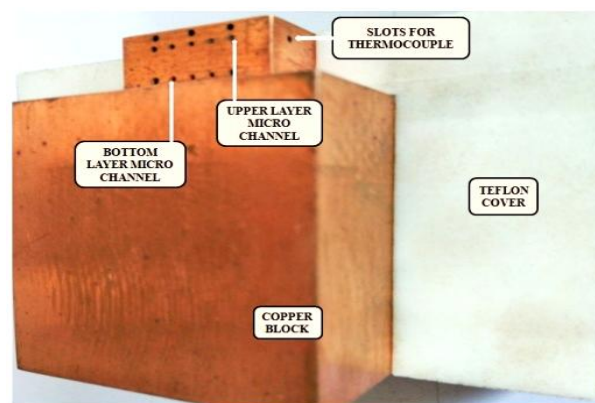


Fig 3. Copper block with Teflon cover

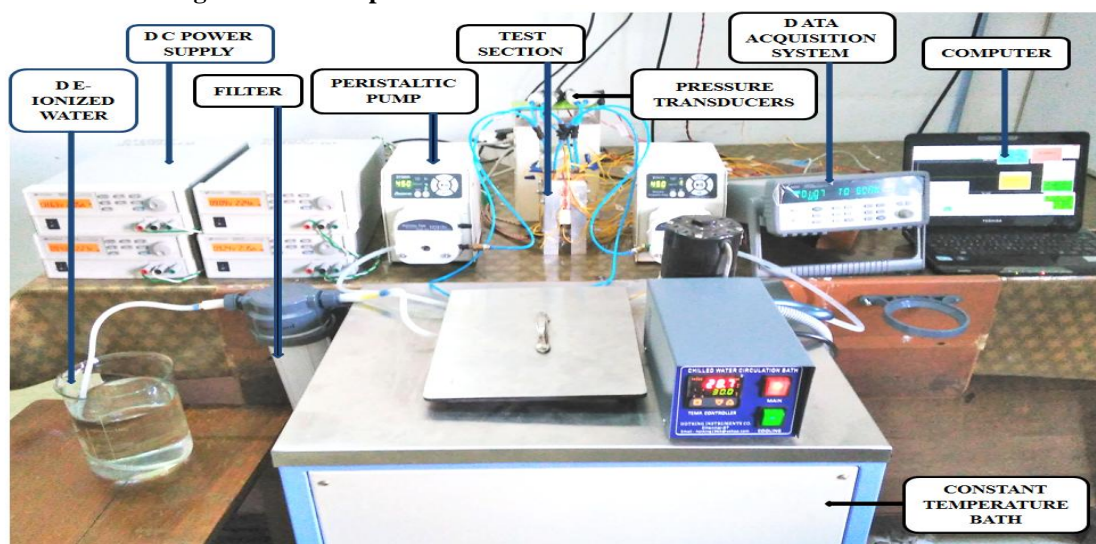


Fig 4. Experimental setup

IV. RESULTS AND DISCUSSION

The numerical and experimental analysis is performed to study the fluid flow and behavior of heat transfer in a double layer circular microchannel heat sink. The lower layer microchannel mass flow rate is taken for plotting all comparisons. Figure 5 shows a change in pressure drop with the mass flow rate through the double layered circular microchannel for different flow arrangements like CF and PF.

Discharge through one microchannel is

$$Q = \frac{A_1 * h}{5t} \quad (7)$$

where A_1 is the area of the cross-section of collecting vessel (m^2) with diameter d_1 in (m), h is the height (m) of the water collected in the collecting vessel and t is the time is taken (sec) for collecting deionized water.

The velocity of the water in (m/s) is

$$u = \frac{Q}{A} \quad (8)$$

where A is the area of cross-section of the circular microchannel with diameter d .

The rate of mass flow through one micro channel is in(kg/s).

$$\dot{m} = \rho Au \quad (9)$$

where ρ is the water density.

Total pressure drop, using equation (10).

$$\Delta P_f = \Delta P_{fL} + \Delta P_{fU} \quad (10)$$

The pressure drop of the lower channel is

$$\Delta P_{fL} = P_{Li} - P_{Lo} \quad (11)$$

where P_{Li} is the lower channel (LC) inlet pressure and P_{Lo} is the LC outlet pressure.

The pressure drop of the upper channel is

$$\Delta P_{fU} = P_{Ui} - P_{Uo} \quad (12)$$

P_{Ui} is the upper channel inlet pressure and P_{Uo} is the upper channel outlet pressure.

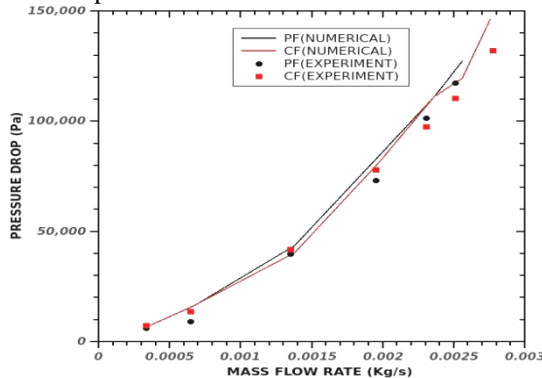


Fig. 5. Change of pressure drop with MFR.

Figure 5 indicates that the pressure drop is found to increase with (MFR). Both in numerical and experimental values of pressure always increases and accord with each other.

The friction factor variation with MFR is shown in Figure 6. Friction factor estimated with the equation (13).

$$f = \frac{2 * \Delta P_f * d}{\rho * L * u^2} \quad (13)$$

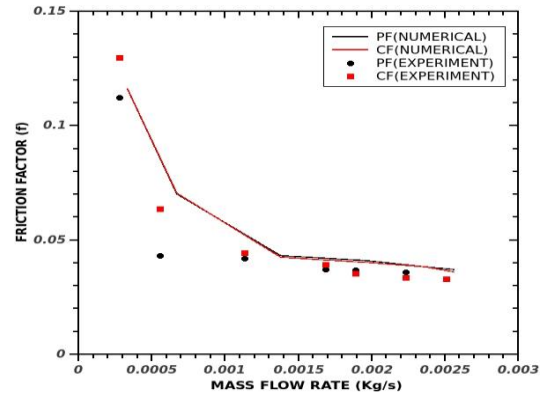


Fig. 6. Change of friction factor with MFR.

The friction factor is found to Down ward trend with the MFR as expected. In the numerical analysis for the CF and PF arrangement, a similar trend is observed. The experimentally calculated friction factor is similar to the numerical results.

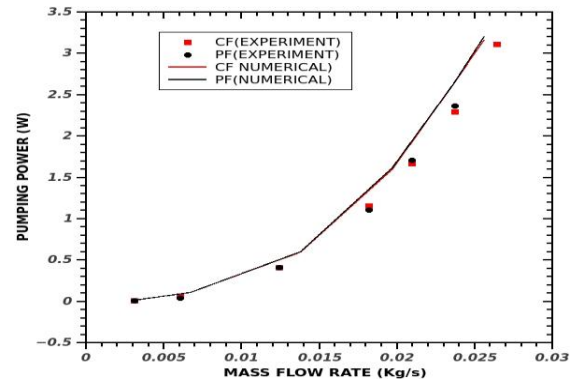


Fig. 7. Change in pumping power with the MFR.

Figure 7 explains the change in pumping power with the MFR through the lower channel.

The pumping power is determined by the relation

$$P = Q * \Delta P_f \quad (14)$$

The pumping power at maximum flow rate in present work is found to be 3 W, which is negligibly small.

Figure 8 represents the change in the fluid outlet temperature in both numerical and experimental analysis. This temperature drops with the mass flow rate of the working fluid.

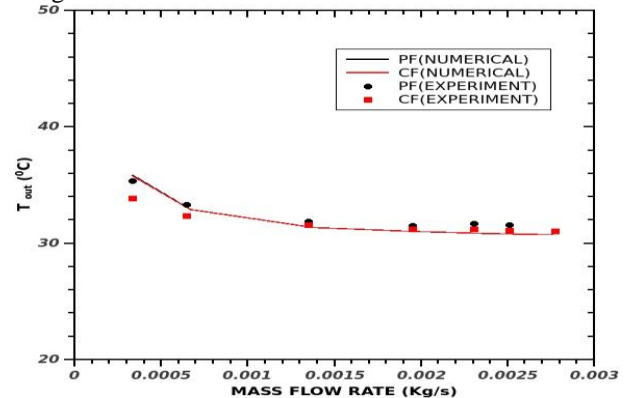
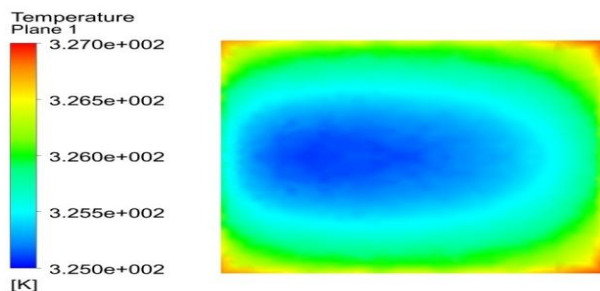
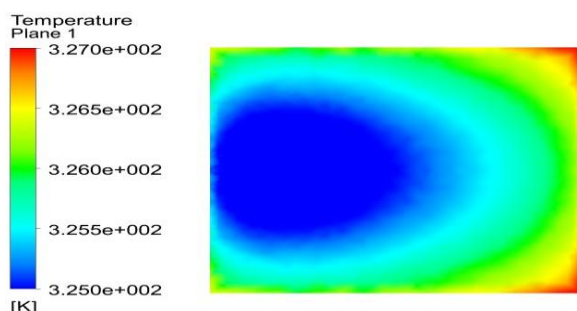


Fig. 8. Change in fluid outlet temperature with the MFR

From Figure 5 and Figure 8 it is seen that both numerical and experimental values nearly same with the counterpart. Therefore the temperature predicted by the numerical analysis at heat sink base should also be same with experimental results.



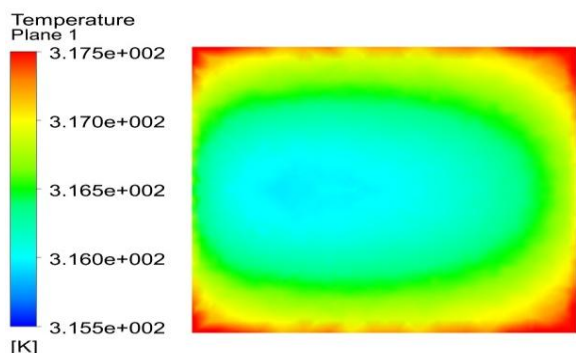
**Fig. 9. Temperature contour at HSB
(Counter flow, 6.69×10^{-4} kg/s)**



**Fig. 10. Temperature contour at HSB
(Parallel flow, 6.69×10^{-4} kg/s)**

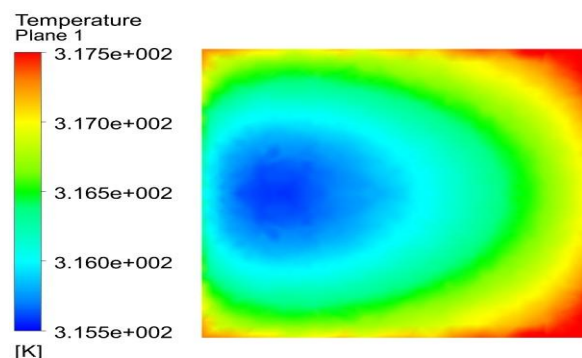
Further analysis was done on the base of the heat sink carried by plotting temperature contours. Figure 9 and 10 shows the temperature contour for low mass flow rate with CF and PF respectively. The results show that the CF arrangement has better uniformity in temperature distribution than the PF arrangement. The higher value of temperature obtained at base of the heat sink is found to be 54°C . This temperature is well below the operating temperature of electronic chips.

Figure 11 and 12 represents temperature contour at the heat sink base for CF and PF respectively for higher flow rates. Parallel flow arrangement has a large variation of temperature as seen in the contour plot in Figure 12. Counterflow has more uniformity in temperature distribution even at higher flow rates. Temperature uniformity is the desired factor to avoid thermal stresses.



**Fig. 11. Temperature contour at HSB
(Counterflow, 25×10^{-4} kg/s)**

The results show that the CF arrangement is always better for all ranges of mass flow rates.



**Fig. 12. Temperature contour at HSB
(Parallel flow, 25×10^{-4} kg/s)**

V. CONCLUSIONS

The pressure drop and thermal aspects of a double-layer circular MCHS estimated using CF and PF arrangement. Numerical and experimental results compared in the present work. The working fluid used is the deionized water. The diameter of microchannel was $700 \mu\text{m}$. Constant heat input of 80W is used for the heating.

Total pressure drop was growing with the MFR of fluid in both numerical and experimental analysis. The numerical results obtained were nearly same with the experimental values. The fluid outlet temperature was also found to be following the experimentally obtained fluid outlet temperature. Therefore it is concluded that numerical analysis mimics the experimental results. Temperature contours at the base of the heat sink are plotted for low and high mass flow rates. The maximum temperature obtained at the heat sink base is found to be 54°C . This is much below the operating temperature of the electronic chips.

Comparison of the temperature contours of CF and PF arrangements show that the CF arrangement has better temperature uniformity than the PF arrangement. This induces less thermal stress on the electronic component resulting in log life of electronics. Therefore it is concluded that the CF analysis has better than the PF analysis.

VI. ACKNOWLEDGMENT

We wish to thank the Technical Education Quality Improvement Programme (TEQIP Phase II) Government of India for supporting this work.

REFERENCES

1. D.B.Tuckerman, R.F.W.Pease. 1981. "High-performance heat sinking for VLSI", IEEE Electron Device Letters EDL-2 P 126-129.
2. T.M.Adams, S.I.Abdel-Khalik, S.M.Jeter, Z.H.Qureshi. 1998. "An Experimental Investigation of single phase forced convection in Microchannels", International Journal of Heat and Mass Transfer 41, P 851-857.

3. Weilin Qu, Issam Mudawar. 2002. "Experimental and numerical study of pressure drop and heat transfer in a single-phase micro-channel heat sink", International Journal of Heat and Mass Transfer 45, P 2549–2565.
4. M.R. Sohel, R.Saidur, Mohd Faizul Mohd Sabri, M.Kamalisarvestani, M.M.Elias, Ali Ijam. 2013. "Investigating the heat transfer performance and thermo physical properties of nanofluids in circular microtubes", International Communications in Heat and Mass Transfer, Vol.42, P 75–81.
5. Amirah M.Sahar, Mehmed R.Ozdemir, Ekhlas M.Fayyadh, Jan Wissink, Mohamed M.Mahmoud, Tassos G.Karayiannis. 2016. "Single phase flow pressure drop and heat transfer in rectangular metallic microchannels", Applied Thermal Engineering Vol.93, P 1324–1336.
6. Paisrn Naphon, Osod Khonseur. 2009. "Study on the convective heat transfer and pressure drop in the microchannel heat sink", International Communications in Heat and Mass Transfer, Vol.36, P 39-44.
7. Wahib Owhaib, Bjorn Palm. 2004. "Experimental investigation of single phase convective heat transfer in circular microchannels" Experimental Thermal and Fluid Science, Vol 28, P 105-110.
8. Ming Li, Tariq S.Khan, Ebrahim Al- Hajri, Zahid H.Ayub. 2016. "Single phase heat transfer and pressure drop analysis of a dimpled enhanced tube", Applied Thermal Engineering, Vol.104, P 38–46.
9. Kambiz Vafai, Lu Zhu. 1999. "Analysis of two layered microchannel heat sink concept in electronic cooling", International Journal of Heat and Mass Transfer. 42 P2287– 2297.
10. Ercan M.Dede, Yan Liu. 2013. "Experimental and Numerical investigation of a multi pass branching microchannel heat sink", Applied Thermal Engineering, Vol. 55, 51-60.
11. N. Lei, P. Skandakumaran, A.Ortega. 2006. "Experimental and Modeling of Multilayer Copper Mini channel Heat sinks in Single –Phase Flow", 0-7803-9524-7/6 IEEE.
12. Behzad Osanloo, Akbar Mohammadi –Ahmar, Ali Solati, Mostafa Baghani. 2016. "Performance enhancement of the double-layered micro channel heat sink by use of tapered channels", Applied Thermal Engineering, Vol 102, P1345-1354.
13. Yuling Zhai, Zhouhang Li, Hua Wang, Jianxin Xu. 2017. "Thermodynamic analysis of the effect of channel geometry on heat transfer in double-layered micro channel heat sinks", Energy Conversion and Management, Vol 143, P431-439.
14. A.F. Ansys 16. User's Guide, Ansys Inc.,2016